Airy-Based Form-Finding of Purely Compressed Masonry Shells Under Vertical and Horizontal Loads

Sam Cocking[1(✉)], Luigi Sibille[2], Sigrid Adriaenssens[3], Americo Cunha Jr[4,5], Francesco Fabbrocino[6], and Carlo Olivieri[3,6]

[1] Department of Engineering, University of Cambridge, JJ Thomson Avenue 7a, Cambridge CB3 0FA, UK
sc740@cam.ac.uk

[2] Department of Ocean Operations and Civil Engineering, Norwegian University of Science and Technology, 4th Floor, A-block, Larsgårdsvegen 2, 6009 Ålesund, Norway
luigi.sibille@ntnu.no

[3] Department of Civil and Environmental Engineering, Princeton University, Princeton, NJ 08544, USA
sadriaen@princeton.edu

[4] National Laboratory of Scientific Computing – LNCC, Petrópolis, Brazil
americo@lncc.br

[5] Rio de Janeiro State University – UERJ, Rio de Janeiro, Brazil
americo.cunha@uerj.br

[6] Department of Engineering, Pegaso Telematic University, Centro Direzionale ISOLA F2, 80143 Naples, Italy
{francesco.fabbrocino,carlo.olivieri}@unipegaso.it

Abstract. The assessment and design of masonry vaulted structures in seismic regions presents challenges to the designer. Typical form-finding methods for compression-only shells may not directly consider horizontal loading, leading to uncertainty regarding structural performance during earthquake events. In the case of new design, this can result in inefficient structures and material overuse, while historic structures may be condemned or damaged through inappropriate interventions. Direct consideration of the static horizontal force capacity - the threshold at which hinge formation triggers dynamic, rocking-like mechanisms in the vault - would allay these concerns, and is primarily a product of the structural geometry. Recent work by the authors has presented a methodology for form-finding compression-only shells under combined vertical and horizontal loading, which is based on the theories of Limit Analysis and Membrane Equilibrium Analysis. However, this method relies on the constrained optimisation of a concave stress potential, which can result in computational challenges. Solutions may be further complicated in the case of vaults containing either cracking damage or intentional geometric discontinuities, such as cross vaults. This paper outlines the key challenges in refinement and implementation of the new form-finding methodology and presents two potential computational solutions, utilising non-convex optimisation and machine learning methods.

© The Author(s), under exclusive license to Springer Nature Switzerland AG 2026
O. Gervasi et al. (Eds.): ICCSA 2025 Workshops, LNCS 15886, pp. 368–380, 2026.
https://doi.org/10.1007/978-3-031-97576-9_25

Keywords: Vault · Shell · Masonry · Form finding · Airy stress function · seismic

1 Introduction

Compression-only shells, such as unreinforced masonry or concrete vaults, offer elegant structural forms and are often found throughout historic architecture. The duality between form and force means that form-finding methods not only enable the design of new shells of this type, under defined loading conditions, but also offer a means of assessing existing vaulted structures. Under vertical gravity loads, there are a variety of techniques available to perform this task [33]. However, when horizontal forces must also be considered, such as in seismic regions, this analysis becomes more complex. Methods such as Tilted Thrust Line Analysis indirectly consider the effect of horizontal body forces (e.g., as in [15]). Recently, a method based on Membrane Equilibrium Analysis (MEA) has been proposed which directly includes these horizontal forces in the equilibrium formulation [25].

Understanding the horizontal force capacity of compression-only shells is critical when they are proposed for construction in seismic regions. While this type of construction is resource-efficient, typically utilising a small structural depth and eschewing modern reinforcement techniques, the topography of elements such as bricks or tiles can nonetheless be tailored to achieve an adequate structural capacity [28]. Specifically, the static horizontal force capacity of compression-only shells, before activation of rocking mechanisms through hinge formation [7,8,11,27], is of interest. Dynamic behaviour following this point is highly sensitive to both the structural response and the specific characteristics of the earthquake, such as the spectral characteristics and maximum ground acceleration. However, the behaviour up to this static limit is largely governed by geometry.

The methodology adopted in this paper, for direct calculation of the static horizontal force capacity of compression-only shells, is based on MEA [1,4,14], the Safe Theorem of Limit Analysis (LA), and the no-tension hypothesis for masonry-like materials proposed by Heyman [16] and adopted by other authors to model unilateral materials [19,20]. It was first presented in [25], in which a typical masonry sail vault was analysed. It has previously been shown [10,26] that, under vertical forces, MEA offers a less conservative and more accurate safety factor than can be achieved by other LA methods based on classical Thrust Line Analysis (TLA) [17,18,22,31], since these alternative approaches consider the shell to be an arch structure and consequently do not include the beneficial effects of biaxial membrane behaviour.

As described fully in [25], the method used here adopts a parametric description of a concave Airy Stress Function (ASF) alongside a finite-element formulation of equilibrium that directly accounts for vertical and horizontal loads. By ensuring concavity of the ASF, the behaviour of the shell remains purely compressive. However, this can result in computational challenges during implementation of the method. This paper discusses these challenges and introduces

two potential solution strategies: Machine Learning techniques to identify optimum ASFs and non-convex optimisation techniques based on the cross-entropy method [9] to improve computational performance.

2 Membrane Equilibrium Analysis Under Vertical and Horizontal Loads

By adopting Heyman's no-tension hypothesis for masonry-like materials, the equilibrium of a compression-only shell can be expressed in terms of geometry, without the need for mechanical properties. MEA extends the familiar concept of a thrust line [16] to that of a thrust membrane, which must lie within the thickness of the shell in order to prevent collapse. Since the membrane must be purely in compression, its generalised stresses must be negative semi-definite. MEA expresses the equilibrium of this membrane in Pucher form [5,29], in terms of two unknown scalar functions for the stress potential and height, i.e., shape, of the membrane, throughout its extent. The choice of an ASF then reduces these equilibrium equations to transverse equilibrium only.

Pucher stresses are the primary variables in these membrane equilibrium equations. These stresses represent the projections of the generalised stresses onto the planform – i.e., the 2D projection of the shell as viewed from above [5,29]. For general shells, the shell geometry and its vertical projection onto the planform can be conveniently expressed in terms of a Monge patch. The natural vector basis associated with this Monge description can be used to transform the generalised membrane stress components in Pucher stresses. For more details of this approach, readers are directed to [2,3]. Here, the third basis vector in the triad is chosen to be normal to the surface of the shell.

Since the two equations related to Pucher stresses describe both the stresses and shape of the shell membrane, either may be chosen as an unknown. For instance, in the assessment of historic structures, the shape is known while the associated load capacity is sought. For the purposes of form-finding, however, the shell's form is chosen as the unknown and expressed in terms of geometric parameters to be optimised. Constrained optimisation is then performed to identify the shell geometry with the highest horizontal load multiplier, under the unilateral constraints of the masonry material.

For more details of the method summarised below, readers are directed to [25].

2.1 Geometry and Loads

Under the action of self-weight and horizontal body forces defined by a load factor $\lambda = \{\lambda_1, \lambda_2\}$, a general shell is shown in Fig. 1 [25]. A membrane surface S contained within the thickness of this shell can be described by a Monge patch, expressed here using the orthonormal triad for a given Cartesian frame $\{O; x_1, x_2, x_3\}$:

$$\{x = x_1 + x_2 + f(x_1, x_2), (x_1, x_2) \in \Omega\}, \tag{1}$$

where $f(x_1, x_2)$ is an arbitrary continuous function of its arguments (x_1, x_2) and defines the shape of the membrane. Ω is the planform of S on the x_1-x_2 plane, having boundary $\partial\Omega$.

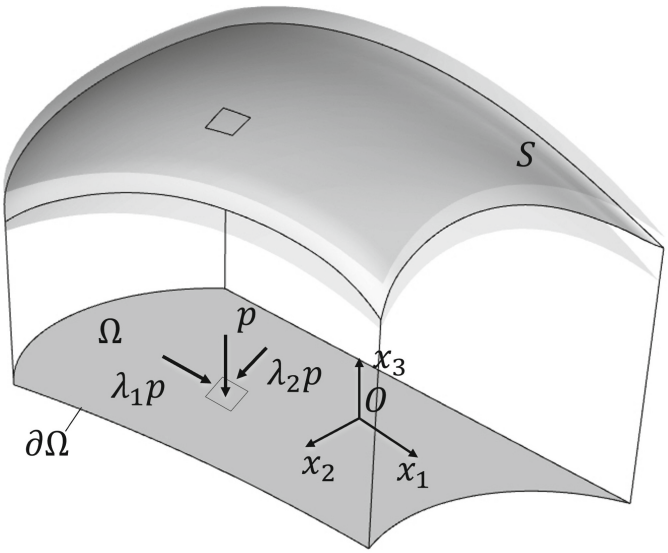


Fig. 1. A general compression-only shell under combined vertical and horizontal body forces. The membrane surface S, fully in compression, lies within the shell thickness and projects onto the planform domain Ω with boundary $\partial\Omega$. The general force components acting on a region of S, form the basis of the membrane equilibrium formulation (from [25]).

Figure 1 shows the general surface forces acting on the shell, per unit projected area of S. These body forces need not be uniform and can be expressed as:

$$p = \{\lambda_1 p, \lambda_2 p, -p\}, \tag{2}$$

where $p = \rho J$ is the self-weight of the shell per unit projected area, given in terms of ρ, the material specific weight, and J, the Jacobian determinant that describes the ratio between surface area on S and projected area on Ω.

2.2 Forces and Equilibrium

Using subscript comma notation (e.g., $\blacksquare_{,ij}$) to represent general derivatives – in this case, subsequent differentiation with respect to the i-th and j-th coordinates

– membrane equilibrium under loads p can be described through a Differential Geometry formulation [3] based on the Pucher stresses [29]. This results in the following three scalar equations:

$$S^{11}_{,1} + S^{12}_{,2} + \lambda_1 \, p = 0, \tag{3}$$

$$S^{21}_{,1} + S^{22}_{,2} + \lambda_2 \, p = 0, \tag{4}$$

$$S^{11} f_{,11} + S^{22} f_{,22} + 2 \, S^{12} f_{,12} + f_{,1} \, \lambda_1 \, p + f_{,2} \, \lambda_2 \, p - p = 0. \tag{5}$$

where S^{ij} is the ij Pucher stress component for $i, j = 1, 2$. By solving these equilibrium equations using a continuous stress potential, the ASF $F(x_1, x_2)$, the following are obtained:

$$S^{11} + \int \lambda_1 \, p \, dx_1 = F_{,22}, \tag{6}$$

$$S^{22} + \int \lambda_2 \, p \, dx_2 = F_{,11}, \tag{7}$$

$$S^{12} = S^{21} = -F_{,12}. \tag{8}$$

$F(x_1, x_2)$ is assumed to be continuous, as discussed in more detail in [21,24]). Adapting these equations, using the definition $h_i = \int \lambda_i \, p \, dx_i$ with $i = 1, 2$, a single linear equation is obtained in which the ASF is unknown:

$$(F_{,22} - h_1) f_{h,11} + (F_{,11} - h_2) f_{h,22} - 2 \, F_{,12} \, f_{h,12} - f_{h,1} \, \lambda_1 \, p - f_{h,2} \, \lambda_2 \, p - p = 0. \tag{9}$$

As described in [25], this second-order PDE may be elliptic, parabolic, or hyperbolic. Here, we assume that Eq. (9) is elliptic and can be formulated as a Boundary Value Problem (BVP), supplemented by conditions on the stress function or on its normal slope with respect to the boundary. In formulating this BVP, either Dirichlet-type boundary conditions, specifying the value of f along the boundary, or Neumann-type, specifying the derivative of f along the outward unit normal $\mathbf{n}$ on the boundary, or a combination of both types, may be used. It is often convenient to use Dirichlet-type conditions to define f along the boundary, based on an initial architectural design for the shell that is being form-found.

2.3 Constitutive Restriction and Requirements of Continuity

As described in [25], the constitutive restriction for a no-tension material such as masonry can be expressed as follows:

$$\mathbf{T} \in \mathrm{Sym}^{-}, \quad \mathbf{E} \in \mathrm{Sym}^{+}, \quad \mathbf{T} \cdot \mathbf{E} = 0, \tag{10}$$

Here, $\mathbf{T}$ is the Cauchy stress tensor, $\mathbf{E}$ is the infinitesimal strain tensor, and Sym^+ and Sym^- are the spaces of symmetric positive and negative semidefinite tensors, respectively. In terms of the ASF, this constitutive restriction can also be expressed as follows:

$$F_{,11} + F_{,22} \leq 0, \quad F_{,11}F_{,22} - F_{,12}^2 \geq 0, \tag{11}$$

Consequently, the curvature tensor of the ASF must be negative semi-definite. In other words, an admissible stress surface must be concave at all points within the domain of interest. The curvature tensor is defined by the Hessian matrix $\mathbf{H}_F$, as follows:

$$\mathbf{H}_F = \begin{bmatrix} F_{,11} & F_{,12} \\ F_{,12} & F_{,22} \end{bmatrix}. \tag{12}$$

Here, the diagonal terms correspond to curvature along the x_1 and x_2 directions, while the off-diagonal terms relate to coupling between these directions.

Furthermore, for single patch shells, C^1-continuity is enforced throughout the domain and at the boundaries. Consequently, no singularities are modelled in the stress field, such as may arise in vaults suffering from cracking damage or which have an inherently discontinuous form, such as cross vaults. In such multi-patch scenarios, the specification of C^1-continuity throughout the domain necessitates additional constraints to enforce this continuity at the patch interfaces.

2.4 Expression of Equilibrium in the Weak Form

The PDEs governing membrane equilibrium (Eqs. (5) and (9)) are numerically solved using the finite element method (FEM). In this paper, this step has been implemented with the Python package FEniCS [6]. Previous work has utilised FEM approaches in Mathematica to demonstrate the feasibility of this approach [23]. FEM requires discretisation of the continuous surface S into finite mesh elements, forming the computational domain in which the PDE is solved. FEniCS supports various mesh element types, such as triangles, quadrilaterals, tetrahedra, and hexahedra for 2D and 3D problems.

FEM necessitates reformulation of the governing PDEs in their weak form [13], to accommodate solutions with lower regularity and reduce the continuity requirements on the approximate solution. To obtain the weak form, the PDE is multiplied by a test function v, belonging to the same function space as the sought solution, and integrated over the planform domain Ω. The standard Galerkin method, used in FEniCS, requires the PDE to contain only first-order derivatives. Hence, integration by parts is applied to reduce the derivative order, resulting in additional boundary terms that vanish due to the Dirichlet boundary conditions.

Following these steps, the equilibrium equation under horizontal loads (Eq. (9)) becomes as follows:

$$\int_{\Omega} \left[\left(F_{,22} - h_1(\lambda_1) \right) f_{,1} v_{,1} + \left(F_{,11} - h_2(\lambda_2) \right) f_{,2} v_{,2} - 2F_{,12} f_{,1} v_{,2} - f_{,1} \lambda_1 pv - f_{,2} \lambda_2 pv - pv \right] \mathrm{d}\Omega = 0. \tag{13}$$

3 Discontinuities in the Masonry Shell - Example of a Cross Vault

As alluded to in Sect. 2.3, it may be desired to generalise the form-finding method to multi-patch scenarios when considering inherent discontinuities in the form of a proposed shell. Cross vaults are a simple and common example of such discontinuity. Inspired by the cross vaults of Kings College Chapel in Cambridge, UK, Fig. 2 shows an initial design with discontinuities along both lines of mirror symmetry in its planform.

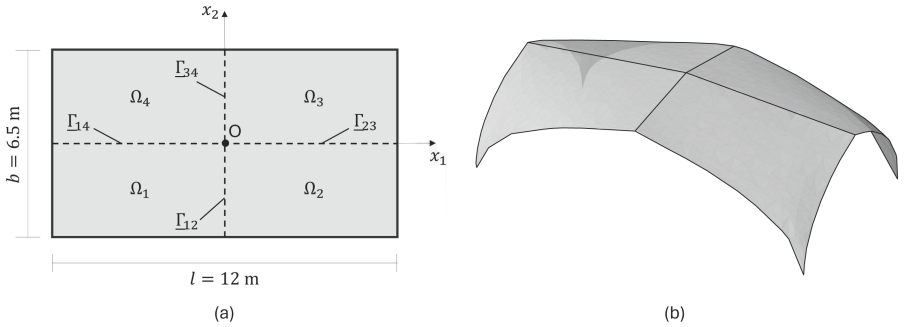


Fig. 2. (a) A rectangular planform domain and (b) the corresponding shell geometry, featuring discontinuities along both lines of mirror symmetry, partitioning the domain into four subdomains $\Omega_{1,2,3,4}$ separated by interfaces $\Gamma_{12,23,34,14}$.

3.1 Airy Stress Function Definition

One appropriate family of ASFs for the multi-patch membrane shown in Fig. 2 can be defined piecewise as follows:

$$\mathcal{F}(\sigma, \alpha, \gamma) = \begin{cases} F_2(\sigma, \alpha, \gamma), & \text{in } \Omega_1 \text{ and } \Omega_3, \\ F_1(\sigma, \alpha, \gamma), & \text{in } \Omega_2 \text{ and } \Omega_4. \end{cases} \tag{14}$$

where F_1 and F_2 are given by:

$$F_1(\sigma, \alpha, \gamma) = \frac{\gamma}{2b^2} \left(\frac{b^2}{4} - x_2^2 \right) + \frac{\sigma - \gamma}{2l^2} \left(\frac{l^2}{4} - x_1^2 \right), \tag{15}$$

$$F_2(\sigma, \alpha, \gamma) = \frac{\alpha}{2l^2}\left(\frac{l^2}{4} - x_1^2\right) + \frac{\sigma - \alpha}{2b^2}\left(\frac{b^2}{4} - x_2^2\right). \tag{16}$$

Here, l and b are constants defining the size of the planform (c.f., Fig. 2), x_1 and x_2 are spatial coordinates, σ, α, and γ are parameters, and Ω_i are the domains of the piecewise regions.

4 Challenges of this Approach

Parameterisation of the family of ASFs requires the use of multiple parameters, posing notable challenges during the form-finding optimisation process, particularly in ensuring concavity of the ASF. Greater sophistication of the family of ASFs can be achieved by increasing the number of parameters. However, this leads to a high-dimensional parameter space, making it more onerous to interpret whether a continuous domain or specific region within the parameter space exists in which concavity is consistently maintained. Concavity is of paramount importance, as it guarantees a purely compressive stress state within the shell in alignment with the no-tension hypothesis commonly assumed for masonry-like materials.

The inherent nonlinearity of the governing equilibrium equations further complicates the numerical solution process. Specifically, the equations relating the parameters of the ASF to the membrane geometry are nonlinear. This creates challenges in achieving convergence and numerical stability, which may result in a poor solution, sensitivity to local minima, or failure of the solver.

These challenges are amplified when the shell structure exhibits singularities, such as geometric discontinuities (see Fig. 2). In these cases, the shell problem is decomposed into multiple patches, each described by separate Airy stress parameters. In this multi-patch approach, continuity of the ASF along the boundary lines between patches must also be enforced. This continuity is essential to maintaining accurate stress transfer and significantly increases both the complexity and computational burden of the overall form-finding process.

Faced with these challenges, it is not straightforward to computationally implement the method outlined above in Sect. 2. Traditional optimisation packages have been trialled in Python and have struggled to perform adequately. In contrast, a tool that utilises these methods will only be of value to practitioners if it can achieve reliable results in efficient run-times. To combat these challenges, the following Sect. 5 outlines potential strategies to improve computational performance and reliability.

5 Potential Solutions and Directions for Future Work

Form-finding with a multi-parameter Airy Stress Function can be approached via two broad strategies: data-driven machine learning (ML) and non-convex optimisation. Each approach aims to identify parameter values that satisfy the equilibrium conditions represented by the governing PDE for a given design

scenario, under the constraints that the chosen ASF is concave and that the form-found membrane must lie within the thickness of the shell.

Within ML approaches, regression-based methods employ supervised learning to predict optimal Airy stress parameters. A dataset of solved examples is generated by varying the parameter set within ranges that guarantee concavity, and recording the optimum membrane solution obtained from the equilibrium equation. Regression algorithms then learn patterns from these datasets without explicitly embedding the underlying physics. Frequently used regression techniques include ensemble methods such as random forests [30], Gaussian process (GP) regression [34], and instance-based methods such as k-nearest neighbours (k-NN) [12].

However, regression-based methods present certain limitations. A notable drawback is their black-box nature, meaning they depend heavily on the quality and diversity of the dataset. They generally perform well within the range covered by training data but may struggle with extrapolation, as they do not inherently respect physical constraints beyond observed scenarios [32]. For example, random forests are confined to predictions within the bounds of their training data [30]. Consequently, if a new scenario significantly differs from those encountered during training, these methods risk providing non-physical or unstable parameter sets.

An alternative ML strategy is the use of Physics-Informed Neural Networks (PINNs), which integrate governing physical equations directly into the training process. Unlike traditional regression models, PINNs embed the equilibrium PDE into their loss function. In this strategy, a neural network (e.g., a feed-forward deep network) is constructed to represent the ASF over the domain [32]. This method allows the PDE itself, supplemented with appropriate boundary conditions, to drive network training without relying exclusively on extensive datasets.

Despite these advantages, PINNs present their own challenges. Training such networks is computationally demanding, requiring iterative adjustment of potentially very many parameters (representing weights and biases in the network) until the PDE residual is successfully minimised. The high dimensionality and non-convex nature of the optimisation pose significant convergence challenges, necessitating careful and extensive tuning [32]. Moreover, since each new design scenario requires training a new network from scratch, unless the network architecture explicitly accommodates multiple cases, the computational overhead can be substantial. Thus, while PINNs enhance physical accuracy and consistency compared to purely data-driven regression methods, they inherently trade off computational efficiency and simplicity for these advantages.

Aside from ML methods, the second major strategy for solving the form-finding problem is direct optimisation using non-convex methods. In contrast to convex optimisation, non-convex methods are better suited to handling local

minima. However, this is often associated with a heavier computational cost. While techniques for non-convex optimisation are often black-box in nature, the use of control variables in some methods such as Cross-Entropy (CE) Optimisation [9] provides improved transparency. The CE method uses rare event estimation to iteratively update a probability distribution over the solution space, converging efficiently to the global optimum. Its flexibility and robustness make it well-suited for handling the multiple constraints and parameters in the form-finding method.

In ongoing work, both ML regression (utilising random forest, gradient boosting, and k-NN) and the CE method are being trialled as implementation routes for the form-finding methodology. Evaluated alongside more traditional optimisation strategies and packages, these approaches show promise for improved reliability and computation time.

6 Conclusions

This paper has summarised a methodology for the form-finding of compression-only shells, which directly considers both vertical and horizontal applied loading. The method is of practical relevance in the design of new shells where horizontal loading is appreciable – such as in seismic areas or regions of high wind loading. Through the use of the Pucher stress formulation, alongside a parametric, concave ASF, optimum thrust membrane geometries can be obtained for various load combinations and used to establish an ideal final structural form. This provides a more effective and intuitive workflow to the designer, compared to other methods which only consider horizontal loading indirectly.

However, the sophistication of the solution is linked to the number of parameters used to define the ASF which, in turn, increases the computational challenge of implementing this method. The inability of no-tension materials such as masonry to sustain tensile stresses manifests in this method in the requirement for the ASF to be concave, further constraining the solution procedure. Moreover, for designs such as cross vaults that exhibit inherent discontinuities of form, the need to achieve continuity of the ASF along the boundaries of a multi-patch solution adds further complexity.

Strategies to overcome these computational challenges have also been outlined in this paper. These can be grouped into two key categories: non-convex optimisation strategies, and Machine Learning techniques which can be trained to achieve viable solutions in place of direct optimisation. Both categories are the focus of ongoing work, as part of the implementation of this form-finding methodology.

Acknowledgments. The authors gratefully acknowledge the financial support of: The Italian Ministry of University and Research (MUR), Research Grant PRIN 2020 No. 2020EBLPLS on “Opportunities and challenges of nanotechnology in advanced and

green construction materials"; The Italian Ministry of University and Research (MUR), Research Grant PRIN 2022 No. 2022TN5M7F on "TReE - Supporting the Transition to Ecological Economy in Italian cities Regeneration: circular model tools for reusing architecture and infrastructures"; and the United Kingdom Engineering and Physical Sciences Research Council (EPSRC) and Department for Transport (Research Grant No. EP/Y024257/1).

References

1. Angelillo, M., Montanino, A., Pandolfi, A.: On the connection between geometry and statically determined membrane stresses in the human cornea. J. Biomech. Eng. **142**(5), 051006 (2020). https://doi.org/10.1115/1.4044742
2. Angelillo, M., Babilio, E., Fortunato, A.: Singular stress fields for masonry-like vaults. Continuum Mech. Therm. **25**, 423–441 (2013). https://doi.org/10.1007/s00161-012-0270-9
3. Angelillo, M., Fortunato, A.: Equilibrium of masonry vaults. In: Novel Approaches in Civil Engineering, pp. 105–111. Springer (2004)
4. Angelillo, M., Fortunato, A., Montanino, A., Lippiello, M.: Singular stress fields in masonry structures: Derand was right. Meccanica **49**, 1243–1262 (2014). https://doi.org/10.1007/s11012-013-9842-z
5. Angelillo, M., Iannuzzo, A., Montanino, A.: Discretised continuum approaches: from continuum to dis-continuum. In: Discrete Computational Mechanics of Masonry Structures, pp. 95–163. Springer (2023). https://doi.org/10.1007/978-3-031-14934-9_4
6. Baratta, I.A., et al.: DOLFINx: the next generation fenics problem solving environment (2023). https://doi.org/10.5281/zenodo.10447666
7. Bisegna, P., Coccia, S., Como, M., Nodargi, N.A.: A novel impact model for the rocking motion of masonry arches. Meccanica **58**(10), 2079–2093 (2023). https://doi.org/10.1007/s11012-023-01675-3
8. Castellano, A., Elia, I., Fraddosio, A., Olivieri, C., Piccioni, M.D.: A new experimental approach for small-scale dynamic tests on masonry arches aimed at seismic assessment. Int. J. Mason. Res. Innov. **7**(1–2), 89–112 (2022). https://doi.org/10.1504/IJMRI.2022.119865
9. Cunha Jr, A., Issa, M.V., Basilio, J.C., Telles Ribeiro, J.G.: CEopt: a MATLAB package for non-convex optimization with the cross-entropy method. PrePrint arXiv:2409.00013 (2024). https://doi.org/10.48550/arXiv.2409.00013. https://ceopt.org
10. Cusano, C., Montanino, A., Olivieri, C., Paris, V., Cennamo, C.: Graphical and analytical quantitative comparison in the domes assessment: the case of San Francesco di Paola. Appl. Sci. **11**(8), 3622 (2021). https://doi.org/10.3390/app11083622
11. De Lorenzis, L., DeJong, M., Ochsendorf, J.: Failure of masonry arches under impulse base motion. Earthq. Eng. Struct. Dyn. **36**(14), 2119–2136 (2007). https://doi.org/10.1002/eqe.719
12. Fix, E.: Discriminatory Analysis: Nonparametric Discrimination, Consistency Properties, vol. 1. USAF school of Aviation Medicine (1985)
13. Fletcher, C.A.J.: Galerkin Finite-Element Methods, pp. 86–154. Springer, Heidelberg (1984). https://doi.org/10.1007/978-3-642-85949-6_3

14. Fraternali, F., Angelillo, M., Fortunato, A.: A lumped stress method for plane elastic problems and the discrete-continuum approximation. Int. J. Solids Struct. **39**(25), 6211–6240 (2002). https://doi.org/10.1016/S0020-7683(02)00479-3
15. Galassi, S., Tempesta, G.: Safety assessment of masonry undamaged and damaged arches subjected to gravitational loads and horizontal forces. a numeric procedure to identify the optimal thrust line. Int. J. Solids Struct. **301**, 112943 (2024). https://doi.org/10.1016/j.ijsolstr.2024.112943
16. Heyman, J.: The stone skeleton. Int. J. Solids Struct. **2**(2), 249–279 (1966). https://doi.org/10.1016/0020-7683(66)90018-7
17. Huerta, S.: Galileo was wrong: the geometrical design of masonry arches. Nexus Netw. J., 25–51 (2006). https://doi.org/10.1007/978-3-7643-8188-2_4
18. Huerta Fernández, S.: Geometry and equilibrium: the gothic theory of structural design. Struct. Eng. **84**(2), 23–28 (2006)
19. Iannuzzo, A., Mallardo, V.: A novel approach to model differential settlements and crack patterns in masonry structures. Eng. Struct. **323**, 119220 (2025)
20. Montanino, A., Iannuzzo, A.: A quadrilateral plate-type finite element to model stress singularities in no-tension materials. Comput. Methods Appl. Mech. Eng. **432**, 117433 (2024)
21. Montanino, A., Olivieri, C., Zuccaro, G., Angelillo, M.: From stress to shape: Equilibrium of cloister and cross vaults. Appl. Sci. **11**(9), 3846 (2021). https://doi.org/10.3390/app11093846
22. Nodargi, N.A., Bisegna, P.: Thrust line analysis revisited and applied to optimization of masonry arches. Int. J. Mech. Sci. **179**, 105690 (2020). https://doi.org/10.1016/j.ijmecsci.2020.105690
23. Olivieri, C.: FORMERLY-Math: constrained form-finding through membrane equilibrium analysis in Mathematica. Softw. Impacts **16**, 100512 (2023). https://doi.org/10.1016/j.simpa.2023.100512
24. Olivieri, C., Angelillo, M., Gesualdo, A., Iannuzzo, A., Fortunato, A.: Parametric design of purely compressed shells. Mech. Mater. **155**, 103782 (2021). https://doi.org/10.1016/j.mechmat.2021.103782
25. Olivieri, C., Cocking, S., Fabbrocino, F., Iannuzzo, A., Placidi, L., Adriaenssens, S.: Seismic capacity of purely compressed shells based on Airy stress function. Continuum Mech. Thermodyn. **1**(1), 1 (2025)
26. Olivieri, C., Fortunato, A., DeJong, M.: A new membrane equilibrium solution for masonry railway bridges: the case study of marsh lane bridge. Int. J. Mason. Res. Innov. **6**(4), 446–471 (2021). https://doi.org/10.1504/IJMRI.2021.118831
27. Oppenheim, I.J.: The masonry arch as a four-link mechanism under base motion. Earthq. Eng. Struct. Dyn. **21**(11), 1005–1017 (1992). https://doi.org/10.1002/eqe.4290211105
28. Paris, V., Pizzigoni, A., Adriaenssens, S.: Statics of self-balancing masonry domes constructed with a cross-herringbone spiraling pattern. Eng. Struct. **215**, 110440 (2020). https://doi.org/10.1016/j.engstruct.2020.110440
29. Pucher, A.: Uber den Spannungszustand in gekrümmten Flächen. Beton und Eisen **33**(19), 298–304 (1934)
30. Segal, M.R.: Machine learning benchmarks and random forest regression (2004)
31. Stockdale, G.L., Sarhosis, V., Milani, G.: Seismic capacity and multi-mechanism analysis for dry-stack masonry arches subjected to hinge control. Bull. Earthq. Eng. **18**(2), 673–724 (2020). https://doi.org/10.1007/s10518-019-00741-4

32. Vahab, M., Haghighat, E., Khaleghi, M., Khalili, N.: A physics-informed neural network approach to solution and identification of biharmonic equations of elasticity. J. Eng. Mech. **148**(2), 04021154 (2022)
33. Veenendaal, D., Block, P.: An overview and comparison of structural form finding methods for general networks. IJSS **49**(26), 3741–3753 (2012)
34. Williams, C., Rasmussen, C.: Gaussian processes for regression. Adv. Neural Inf. Process. Syst. **8** (1995)